

Alma Mater Studiorum Università di Bologna
Archivio istituzionale della ricerca

Investigation of water state during induced crystallization of honey

This is the final peer-reviewed author's accepted manuscript (postprint) of the following publication:

Published Version:

Tappi S., Laghi L., Dettori A., Piana L., Ragni L., Rocculi P. (2019). Investigation of water state during induced crystallization of honey. FOOD CHEMISTRY, 294, 260-266 [10.1016/j.foodchem.2019.05.047].

Availability:

This version is available at: <https://hdl.handle.net/11585/689236> since: 2021-10-08

Published:

DOI: <http://doi.org/10.1016/j.foodchem.2019.05.047>

Terms of use:

Some rights reserved. The terms and conditions for the reuse of this version of the manuscript are specified in the publishing policy. For all terms of use and more information see the publisher's website.

This item was downloaded from IRIS Università di Bologna (<https://cris.unibo.it/>).
When citing, please refer to the published version.

(Article begins on next page)

Investigation of water state during induced crystallization of honey

Silvia Tappi¹, Luca Laghi^{1,2*}, Amanda Dettori², Lucia Piana³, Luigi Ragni^{1,2}, Pietro Rocculi^{1,2}

¹Interdepartmental Centre for Agri-Food Industrial Research, *Alma Mater Studiorum*, University of Bologna, Piazza Goidanich 60, 47521 Cesena (FC), Italy

²Department of Agricultural and Food Science, *Alma Mater Studiorum*, University of Bologna, Campus of Food Science, Piazza Goidanich 60, Cesena (FC), Italy

³Piana Ricerca e Consulenza, Castel San Pietro Terme, Bologna.

* Corresponding author. E-mail address: to l.laghi@unibo.it

Abstract

This work studied water state of honey during crystallization, obtained statically and dynamically, by differential scanning calorimetry (DSC), water activity (a_w) assessment and time domain nuclear magnetic resonance (TD-NMR).

Crystallization was induced by adding 5% of crystallized honey to three honey samples with different fructose/glucose ratio, the key characteristic for honey crystallization. Samples were stored at 14 °C. Dynamic crystallization was obtained by using an impeller. DSC showed that the dynamic crystallization was faster than the static one, the latter characterized by two phases, showing different rates. The crystallization rate did not affect a_w , that remained below 0.600. TD-NMR allowed to separately observe two kinds of protons, both pertaining to liquid sugars, one chemically exchanging with water and one not exchanging with it. The combination of techniques allowed speculating that the two crystallization methods led to crystals of different size and shape.

Keywords

Differential scanning calorimetry; dynamic crystallization; Honey; static crystallization; time-domain nuclear magnetic resonance; water activity; water state

Introduction

Honey is a supersaturated solution that contains mainly glucose and fructose (70-80%) and only small amounts of other sugars. The crystallization, or granulation, of honey is a natural phenomenon that occurs during storage and involves only glucose, as fructose is characterized by a higher solubility value.

The rate of crystallization depends on many factors, among which amount of glucose, fructose and water, temperature, glucose supersaturation level, viscosity and presence of pre-formed crystals or impurities (Conforti, Lupano, Malacalza, Arias, & Castells, 2006; Venir, Spaziani, & Maltini, 2010).

Nucleation can be classified as primary or secondary. Primary nucleation occurs when the system does not contain any pre-formed crystal and an energy barrier has to be overcome for the formation of new nuclei. Collision among molecules in the solution leads to the formation of clusters that, if sufficiently big, can overcome the energy barrier and become stable (Hartel, 1993). Higher supersaturation levels increase the probability for clusters to overcome the critical dimension. The secondary nucleation can occur only when pre-existing crystals are present. A secondary crystal can be generated from dendritic growth on the surface of a primary nucleus or when a primary nucleus collides with another primary nucleus or with other components of the system, such as the walls of the vessel (Hartel, 1993).

Guided or induced static crystallization (1,987,893, 1935) is based on the secondary nucleation phenomena and involves the introduction of fine seed crystals that will act as primary crystallization nuclei into liquid honey. Such procedure on one side allows to obtain finely granulate honey, on the other side avoids both unpredictable changes in the texture of honey during storage and crystallization defects (Dettori, Tappi, Piana, Dalla Rosa, & Rocculi, 2018).

Dynamic crystallization (Gonnet, 1994) consists in carrying out the guided crystallization under a slow manual or automatic stirring of the mass for a few days, to impart creaminess and spreadability to the crystallized product. Honey obtained in this way is defined as creamy honey and its peculiar rheological characteristics are due to the formation of very small crystals (Karasu, Toker, Yilmaz, Karaman, & Dertli, 2015). The crystallization rate and rheological characteristics of honeys have been investigated by many works in relation to composition and crystallization levels (Slavomir Bakier, 2007; Sławomir Bakier, Miastkowski, & Bakoniuk, 2016; Conforti et al., 2006; Dobre, Georgescu, Alexe, Escuredo, & Seijo, 2012; Venir et al., 2010). However, to the best of our knowledge, the differences between static and dynamic crystallization have never been investigated before.

In addition, the works published on honey have rarely addressed the behavior of water during crystallization, beyond the mere observation of water activity (Gleiter, Horn, & Isengard, 2006; Zamora & Chirife, 2006). Water activity determines honey microbiological stability during storage. It is deeply influenced by crystallization because glucose binds six molecules of water in liquid honey, but crystallizes mainly in the monohydrate form. Crystallization thus promotes water concentration in the liquid phase, leading in turn to an increase of water activity, allowing the growth of osmophilic yeasts (Gleiter, Horn, & Isengard, 2006).

DSC measurements have been successfully applied to evaluate the crystallization of honey by various authors (Al-Habsi, Davis, & Niranjan, 2013; Venir et al., 2010), who measured the amount of glucose crystals on the basis of their melting enthalpy. Transverse relaxation time (T_2) of the protons observed by TD-NMR has been found able to give precious information about water interaction with solutes and sample's structures in several food matrices (Mauro et al., 2016; Petracci et al., 2012). These interactions have been also studied in honey during crystallization, where they have even been used to assess product adulterations through water state (Ribeiro et al., 2014; Ribeiro et al., 2014).

The aim of the present study is to apply differential scanning calorimetry (DSC), water activity and time domain nuclear magnetic resonance (TD-NMR) measurements to investigate the behavior of water in honey during induced crystallization carried out in a traditional static manner or during a dynamic process, achieved through constant stirring of the mass at the optimal crystallization temperature (14 °C).

Material and methods

Raw material and preparation of static crystallization samples

The honey samples used in the present study were selected with the aim of having specific F/G ratios of approximately 1.05, 1.20 and 1.40, leading to fast (FC), medium (MC) and slow (SC) crystallization, respectively (Dettori et al., 2018). Before the experiment of crystallization kinetics, samples were gently heated up to 50 °C to melt any pre-formed crystal. The absence of glucose crystals was evaluated by optical microscopy. The crystal nuclei used were obtained by citrus honey finely granulated, added to the three samples so to reach 5% of the total mass. The so obtained mix was manually stirred with a spatula at room temperature for 10 min. Samples were analyzed for water (at 20 °C with an Abbe refractometer) and sugars content (DIN-NORM-10758, 1997). During static crystallization, sampling itself could break the crystalline structure. To limit this confounding factor,

liquid honey added with crystal nuclei and stirred was poured into samples holders ready for each analytical determination. Samples, created in triplicate, were stored in a climatic chamber at 14 °C throughout the entire crystallization process. Storage time needed for complete crystallization of each sample was assessed by means of preliminary tests. Sampling intervals were then adjusted accordingly, as follows: 0, 2, 7, 9, 22, 43 and 50 days for the FCs samples; 0, 10, 15, 34, 51 and 62 days for the MCs samples; 0, 7, 14, 21, 28, 34, 41, 48, 63, 83 and 102 days for the SCs samples.

Raw material and preparation of dynamic crystallization samples

Samples were subjected to dynamic crystallization with an in-house made steel temperature controlled stirrer, equipped with a helical impeller having a diameter of 100 mm and rotating at 14 rpm. The mixing chamber (about 1.2 L of volume) was externally cooled with a flux of water/ethylene glycol fluid, so to grant a stirred sample temperature of 14 °C. To create the samples, liquid honey at room temperature was added with 5% (w/w) of crystallized honey and placed in the stirring chamber. Every sample took 3 to 4 hours to reach 14 °C. The moment when the 14 °C were reached was considered as T_0 for the analysis. Samples were collected from the stirring chamber without interrupting the process. Storage durations were determined for each sample through preliminary tests and were of 10, 16 and 32 days for samples FCd, MCd and SCd, respectively. Sampling intervals were 0, 1, 2, 4, 7, 8 and 10 days for the FCd samples; 0, 1, 2, 3, 5, 7, 9, 12, 14 and 16 days for the MCd samples; 0, 2, 3, 4, 7, 9, 11, 14, 18, 21, 25, 28 and 32 days for the SCs samples.

Differential Scanning Calorimetry

Thermal analysis was carried out by differential scanning calorimetry using a DSC Q20 (TA Instruments, Germany) equipped with a cooling unit (TA-Refrigerated Cooling System90). Heat flow and temperature calibration were performed with distilled water (T_m 0.0 °C) and indium (T_m 156.60 °C) under a dry nitrogen flow of 50 mL min⁻¹.

Honey samples were weighed in 50 µl aluminium DSC capsules and sealed. At each sampling time, three replicates were analyzed through temperature scanning at 5 °C/min from 14 to 100 °C.

Peaks were integrated with the Software TA-Universal analyzer, determining melting temperature (T_m) and enthalpy (ΔH) of the granulated honeys.

Water activity (a_w)

Water activity was measured with an ACQUA LAB Water Activity Meter, (Decagon Devices, US).

116 For statically crystallized honey, three samples holders were filled with liquid honey at the beginning
117 of the storage, then measured at each sampling time. Between measurements, samples were covered
118 with lids and protected with parafilm. For dynamically crystallized honey, samples were collected at
119 each sampling time.

120 **TD-NMR**

121 The transverse relaxation time (T_2) of protons was measured at 25 °C with the Carr–Purcell–Meiboom–
122 Gill (CPMG) (Meiboom & Gill, 1958) pulse sequence (Ribeiro et al., 2014; Ribeiro et al., 2014), using
123 a Bruker Minispec PC/20 spectrometer (Bruker, Germany) working at 20 Hz. The exponential decay
124 comprised 3200 echoes, an echo time (TE) of 0.080 ms, leading to a dead time of 167 μ s, and a recycle
125 delay of 5 s. The number of scans and the amplification factor were chosen so that a S/N ratio value of
126 300 was reached, while signal clipping was prevented. Data mining was performed in R computational
127 language (R Development Core Team, 2011), by means of routines developed in-house. In order to
128 treat honey as a two components system, by following de Ribeiro *et al.* (Ribeiro, Mársico, Carneiro,
129 Monteiro, Júnior, et al., 2014), the phased experimental curves were fit towards the sum of two
130 exponential decays, according to the equation:

$$S_{(t)} = \sum_{i=1}^N I_n e^{\left(\frac{-t}{T_{2,n}}\right)} + E_{(t)}$$

131 where I_n represents the intensity of each proton population and $T_{2,n}$ its transverse relaxation time.

132 The presence of two water populations postulated by Ribeiro *et al.* could be doubted by the massive
133 work by Brown (Brown, 1989), who demonstrated that the sum of two exponential curves fit nicely
134 also the signal of a single water population. This happens when water covers a wide range of relaxation
135 rates, a common case in food matrices (Iaccheri et al., 2015; Laghi et al., 2005; Petracci et al., 2014),
136 thus giving the false impression of two water components. For this reason the T_2 decays, centered and
137 scaled to unity variance, were also employed to build a robust principal component analysis (rPCA)
138 (Hubert, Rousseeuw, & Vanden Branden, 2005) model. This was done by setting an alpha value of
139 0.75. For this model, we calculated the scoreplot, the projection of the samples in the PC space, tailored
140 to highlight the underlying structure of the data. Besides, we calculated the Pearson correlation plot,
141 relating the concentration of each variable to the model components.

142 **Statistics**

143 Differences among samples at specific time-points were looked for by anova test, with Tukey as a post-
144 hoc test, by taking advantage of the aov function of the R package “stats” (Chambers, Freeny, &
145 Heiberger, 1992).

146 For TD-NMR data, differences in the overall trends characterizing the FCs, MCs and SCs samples
147 along storage time were looked for by two-way anova test, followed by Tukey as a post-hoc test. The
148 limited number of samples per point was considered by applying the tests on ranks (Conover & Iman,
149 1981). Intensity and T_2 of each proton population and score values in the rPCA (Hubert et al., 2005)
150 model registered along time were interpolated by means of non-parametric functions. For the purpose,
151 a local regression model was applied, by taking advantage of the loess function (Cleveland, Grosse, &
152 Shyu, 1992) of the R package “stats”, with degree of smoothing equal to 0.9 and the degree of the
153 polynomial equal to 1.

154 **Results and discussion**

155 **DSC**

156 The precise composition (after crystal nuclei addition) of the samples fast (FCs), medium (MCs) and
157 slow (SCs) static crystallization is reported in Table 1. Slight differences were observed between each
158 of the couples of samples grouped as FC, MC or SC. However, the selection allowed to obtain very
159 similar fructose/glucose ratio, the parameter the mostly affecting the crystallization rate.

160 The detailed evolution of the melting enthalpy during static and dynamic crystallization is reported in
161 figure 1, while overall features of the crystallization processes are reported in table 2.

162 The melting enthalpy is proportional to the amount of crystallized glucose, so that at T_0 its value
163 reflects the amount of finely crystallized honey added as starter. FC, MC and SC samples stored
164 statically reached the maximum crystallization values of 34.72, 27.62 and 21.68 J/g, respectively.
165 These values were proportional to the glucose supersaturation level, hence to the amount of glucose
166 that could crystallize (Dettori et al., 2018). Glucose supersaturation level determined also the
167 crystallization rate, so that FCs, MCs and SCs samples reached the maximum melting enthalpy in 50,
168 90 and 102 days, respectively.

169 Although dynamic crystallization is known to increase granulation rate, to our knowledge, no previous
170 study has actually compared the crystallization behavior of honey according to static and dynamic
171 crystallization process. Results obtained showed for the first time that the dynamic process boosted

significantly the crystallization rate, which was 5 to 6 fold faster than the static counterpart. In detail, full crystallization was reached in 10, 16 and 35 days for FCd, MCd and SCd samples, respectively. This was expected, as the nucleation process (both primary and secondary) is known to be strongly increased by inputs of energy into the system, here represented by the mechanical energy given by continuous mixing. According to Hartel (Hartel, 1993), the reason is that an external energy input promotes random energy fluctuations, represented by local concentrations of sugar exceeding the critical value for nucleation. Moreover, agitation promotes the forced migration of molecules, so to reduce the hindrance to mass transfer given by viscosity.

It is possible to notice from figure 1 that, in statically stored samples, the crystallization kinetic showed a linear trend along the entire process, but with an inflection occurring after 9, 15 and 21 days in FCs, MCs and SCs samples, respectively, corresponding to the 50-60% of the process. A similar result was observed by Venir *et al.* (Venir et al., 2010) in *taraxacum* honey. In particular, they observed a change of slope after the crystallization of 15% of glucose, corresponding to the 60 % of the total glucose that could undergo crystallization.

Following Serra-Bovehì (Serra-Bonvehì, 1974), the two stages observed by us and Venir *et al.* (2010) could be ascribed to the alternation of nucleation and crystal growth. The two phenomena can occur simultaneously, but at different rates in relation to the supersaturation level. At the beginning of the process, when supersaturation is high, the formation of new crystals is faster than their growth. As the crystallization proceeds, the nucleation rate decreases exponentially, so that, in a second stage, the predominant process is the enlargement of the existing nuclei.

The two-phase behavior could not be observed in honey samples crystallized dynamically, that instead showed a linear increase of melting enthalpy along the entire storage time. This observation could be rationalized by considering that the energy input represented by the stirring promotes the formation of nuclei, while the constant movement of the mass inhibits the excessive growth of the crystals.

Hence, the different crystallization method adopted not only noticeably influenced the crystallization rate, but it also promoted changes in the formation of crystals that is at the basis of the difference in the rheological properties, as described by Gonnet (1994).

Water activity

Figure S1 reports the evolution of a_w in honey samples statically and dynamically stored as a function of melting enthalpy. Initial values ranged between 0.490 and 0.550. Differences were likely to be caused by the different concentration of sugars and water in the honey samples. Indeed, as shown in

203 table 1, water content varied in the 16.0 - 17.7% range. Values of a_w increased systematically with the
204 amount of crystallized glucose. In detail, the observed changes in a_w were in the 0.3-0.6 range, in
205 agreement with previous investigations (Zamora & Chirife, 2006) carried out on 49 different honey
206 samples. However, in all cases, the final value never exceeded 0.60, the threshold usually considered
207 for osmophilic yeast growth.

208 Contrarily to the melting enthalpy, the increase in a_w followed a linear trend for statically stored
209 samples, with no evident change of slope. This could be explained by considering that water activity
210 depends on the overall characteristics of the samples, failing to discriminate fine differences in the state
211 of water throughout the sample itself.

212 **TD-NMR: two components model**

213 By following the works of Ribeiro *et al.* (Ribeiro et al., 2014; Ribeiro et al., 2014), T_2 weighted TD-
214 NMR signals were fit to a model postulating the possibility to separately observe two protons pools,
215 that were named T_{21} and T_{22} (Fig. 2). Analysis of variance showed that, for both T_2 and intensity of the
216 two populations, level of supersaturation and time had in each case a statistically significant effect
217 ($p < 0.001$). To grab the trends of the two populations along storage in a non-parametric fashion,
218 smoothing trends were calculated. The main features of the so evidenced trends are summarized in
219 table 3.

220 In agreement with Ribeiro *et al.* works, the two protons pools had, at T_0 in the statically crystalized
221 samples, T_2 values around 1.5 and 5 ms respectively. Their relative intensities were found in the
222 present work to be around 55% and 45%. Ribeiro *et al.* ascribed the two populations exclusively to
223 water differently interacting with crystals, but such ascription seems very unlikely, because it does not
224 consider the remarkable number of protons of the sugars. A few qualitative considerations drive the
225 point.

226 In liquid honey, each mole of water brings 0.11 moles of protons. Each mole of glucose or fructose is
227 characterized by 0.028 moles of protons pertaining to -OH groups. Around 75% of them (0.021 moles)
228 was found to be labile (Fabri, Williams, & Halstead, 2005). The exchange rate of these protons
229 between water and sugars is expected (B. Hills, 1998; Venturi et al., 2007) to be much higher than the
230 NMR signal registration rate, reasonably far above 100 s^{-1} (Fabri et al., 2005). In this regime, water and
231 labile sugar protons are observed as a single population. Such population can be simply called
232 “exchangeable”, as suggested by Petracci *et al.* (Petracci et al., 2014) on a different matrix. The

233 remaining sugar protons bound to carbons plus the non-labile –OH protons (accounting for 0.046
 234 moles) cannot exchange with water, so that they can be called “non-exchangeable”.
 235 According to the above considerations, in the samples we have analyzed in the present work, non-
 236 exchangeable and exchangeable protons populations may contribute to T_2 weighted TD-NMR signals
 237 with about a 50:50 relative intensity. Such qualitative consideration is in very good agreement with the
 238 ratio measured in SC samples (51.47:48.53), while it shows a 17.14% discrepancy in the case of FC
 239 samples.
 240 The pool of exchangeable protons is expected to have longer T_2 values, according to the following
 241 reasoning. The T_2 of a proton pertaining to liquid sugar is reasonably in the range of milliseconds.
 242 When this proton is exchanged between sugar and water its T_2 is the weighted average of the T_2 of the
 243 two sites, according to the Carver and Richards (Carver & Richards, 1972), corrected by Hills and
 244 coworkers (B. P. Hills, Wright, & Belton, 1989). Such T_2 is undoubtedly longer than the one of non-
 245 exchangeable protons, because water has been found liquid even in a glassy matrix (B. P. Hills &
 246 Pardoe, 1995), what translates into T_2 in the range of hundreds of milliseconds. According to this
 247 consideration, we therefore suggest that the populations originally named T_{21} and T_{22} by Ribeiro *et al.*
 248 can be ascribed to non-exchanging and exchanging protons, respectively.
 249 Along the entire storage period the two protons pools model was able to fit nicely the T_2 weighted
 250 signals registered on every sample, even on those where crystallization has occurred massively. This
 251 suggests that the liquid fraction of honey had the major, if not the exclusive, contribution to the NMR
 252 signal. Indeed, the CPMG pulse sequence we employed had an unavoidable dead time of 167 μ s. The
 253 protons pertaining to the crystals were expected to be largely unobservable, because characterized by a
 254 T_2 of a few microseconds (B. P. Hills & Pardoe, 1995).
 255 Interestingly, as already observed for the increase of melting enthalpy, for each of the studied samples
 256 two distinct stages of crystallization could be noticed from a T_2 point of view. However, the change
 257 was observed at different times. The first stage could be considered as complete at days 30, 50 and 66
 258 for FCs, MCs and SCs samples, respectively. During this stage, the relative intensity of non-
 259 exchangeable protons population decreased by 8.7%, 7.6% and 4.6% in the FCs, MCs and SCs
 260 samples, respectively. In parallel, the T_2 of non-exchangeable protons increased by 74% to 200%,
 261 while the T_2 of exchangeable protons increased by 10% to 45%. The main contribution to the trends of
 262 both relative populations and T_2 values in the first stage is very likely the subtraction of glucose from
 263 the liquid fraction due to crystallization, leading to an increased concentration of water, as noticed by
 264 Dettori *et al.* (Dettori et al., 2018). Indeed, an increase in water concentration increases the amount of

the exchangeable protons in the system ($\approx 53\%$). As confirmation, the FCs samples, with a higher supersaturation index, showed also the largest and quickest increase of exchangeable protons, followed, proportionally, by MCs and SCs samples. Moreover, the increase of water concentration in the liquid fraction has two further effects. First, it moves the weighted average of T_2 of the exchangeable protons towards higher values. Second, it increases the tumbling rate of the molecules, leading to higher T_2 values for both exchangeable and non-exchangeable protons (Bordoni et al., 2014).

The second stage of static crystallization highlighted by T_2 weighted signals started around day 30, 50 and 66 for samples FCs, MCs and SCs, respectively. This stage was characterized by a partial inversion of the previous trends, with an increase of non-exchanging protons and with a shortening of the T_2 values of both populations. The most likely rationalization of this phenomenon is that the crystals were so densely spread across the entire honey volume that a high percentage of the still liquid molecules interacted with them. Even if it is not possible to describe rigorously such interaction, it probably comprised a reduced mobility, leading to shorter T_2 values, and a less effective sugar-water protons exchange, that increased the number of non-exchanging protons. A confirmation seems to be devised in the fact that the highest reduction of T_2 values and exchanging protons occurred in the FC samples, characterized by the highest amount of crystallized sugar, what translates into a higher solid-liquid interface. In addition, at the liquid-solid interface local gradients of the magnetic fields form, thus leading to shorter T_2 values (Dunn, 2002), linked to the dimension and the shape of the crystals.

Dynamically crystalized samples did not show appreciable differences from the statically crystalized counterparts at T_0 . The dynamic crystallization process showed the same overall features of the first stage of static crystallization, with an increased concentration of exchangeable protons and an increased T_2 values for both populations for each level of glucose supersaturation. The remarkable feature of these trends is the entity of the changes. While the first stage of static crystallization, when crystal nucleation is favoured, leads to a decrease in the pool of non-exchangeable protons of 8.7%, 7.6% and 4.6% for FC, MC and SC samples respectively, dynamic crystallization leads in the same samples to a reduction of 9.8%, 15% and 5.8%. Differences even more clear could be noticed for T_2 values. As an example, while the T_2 of non-exchangeable protons increased for FC, MC and SC samples by 80.9%, 56.9 and 26.4% as a consequence of static crystallization, the same values increased by 198.2%, 114.3% and 74%, respectively, as a consequence of dynamic crystallization. Interestingly, stirring made the values of dynamically crystalized MC and SC samples change similarly to FC samples. This suggests that at the base of the phenomenon is the number of crystals, which it is higher in the samples crystalized dynamically.

297 **TD-NMR: model-free analysis**

298 In order to employ T_2 weighed NMR signals to gain information on the samples without applying a
299 priori determined model, robust principal component analysis (rPCA) (Hubert et al., 2005) was applied
300 on the centered and scaled signals points (Figure 3). In the scoreplot (Figure 3A), the samples spread
301 with storage time along PC 1, which represented 96.8% of the total samples variance.

302 The samples that the two components model identified as collected at the end of the first stage of static
303 crystallization appeared at negative values along PCA, while samples freshly prepared or collected at
304 the end of crystallization were characterized by high and intermediate scores, respectively. This made
305 the pattern covered by the samples along PC 1 undoubtedly similar to those highlighted by the two
306 protons pools model. Again similarly to the two protons pools model, the samples collected at the end
307 of the dynamic crystallization were located at scores that were far lower than the corresponding created
308 with static crystallization. The correlation between the points of the T_2 weighted signals and their
309 importance over PC1 (Figure 3C) showed, in agreement with the two components model, that in the
310 fresh samples the non-exchangeable protons played the highest role, while the opposite was observable
311 at the end of the first stage of crystallization.

312 The non-parametric approach constituted by the rPCA model directly calculated on the signals
313 registered by TD-NMR confirmed, from a protons T_2 point of view, that the static crystallization could
314 be divided into two stages, the second of which partly reversing the effects of the first one. From a T_2
315 point of view, the interactions between crystals and liquid honey seemed of similar type but of different
316 extent for statically and dynamically crystallized samples.

317 **Conclusions**

318 The water behavior in honey during induced crystallization according to static and a dynamic process
319 was investigated.

320 DSC measurements confirmed that the constant movement of the honey during storage decreased the
321 time necessary for the complete crystallization of all the honey types by 5-6 fold. Static crystallization
322 showed two main phases of crystal genesis, identified both by DSC and TD-NMR measurements,
323 characterized by different rates, probably related to the nucleation and crystal growth phases
324 alternation. On the contrary, dynamic crystallization was characterized by a linear trend that was
325 attributed to a prevalence of the nucleation phenomenon over the growth of crystals. Moreover, the
326 crystallization rate did not influence the a_w increase, that remained below 0.600.

327 Through TD-NMR two populations of protons were identified and attributed to liquid sugars protons
328 exchanging and non-exchanging with water. The interaction between crystals and liquid honey showed
329 some differences according to the type of crystallization process adopted, that could be due to the
330 different number and size of the crystals. However, further investigation is necessary to confirm this
331 hypothesis.

332 In general, the described multi-analytical approach confirmed the suitability of the different techniques
333 to study the water mobility in differently crystalized honey, giving integrative results able to increase
334 the knowledge of these complex phenomena with a different level of detail.

335 **Acknowledgements**

336 The authors declare no conflicts of interest

337

338 **Bibliography**

- 339 Al-Habsi, N. A., Davis, F. J., & Niranjana, K. (2013). Development of Novel Methods to Determine Crystalline
340 Glucose Content of Honey Based on DSC, HPLC, and Viscosity Measurements, and Their Use to Examine
341 the Setting Propensity of Honey. *Journal of Food Science*, 78(6). <https://doi.org/10.1111/1750-3841.12103>
- 342 Assil, H. I., Sterling, R., & Sporns, P. (1991). Crystal control in processed liquid honey. *Journal of Food*
343 *Science*, 56(4), 1034–1034. <https://doi.org/10.1111/j.1365-2621.1991.tb14635.x>
- 344 Bakier, S. (2007). Influence of temperature and water content on the rheological properties of polish honeys.
345 *Polish Journal of Food and Nutrition Sciences*, 57(2 (A)), 17–23. [https://doi.org/10.1590/S1516-](https://doi.org/10.1590/S1516-35982010000800027)
346 [35982010000800027](https://doi.org/10.1590/S1516-35982010000800027)
- 347 Bakier, S., Miastkowski, K., & Bakoniuk, J. R. (2016). Rheological properties of some honeys in liquefied and
348 crystallised states. *Journal of Apicultural Science*, 60(2), 153–166. <https://doi.org/10.1515/JAS-2016-0026>
- 349 Bordoni, A., Laghi, L., Babini, E., Di Nunzio, M., Picone, G., Ciampa, A., ... Capozzi, F. (2014). The
350 foodomics approach for the evaluation of protein bioaccessibility in processed meat upon in vitro digestion.
351 *Electrophoresis*, 35(11), 1607–1614. <https://doi.org/10.1002/elps.201300579>
- 352 Brown, R. J. S. (1989). Information available and unavailable from multiexponential relaxation data. *Journal of*
353 *Magnetic Resonance (1969)*, 82(3), 539–561. [https://doi.org/10.1016/0022-2364\(89\)90217-5](https://doi.org/10.1016/0022-2364(89)90217-5)
- 354 Carver, J. P., & Richards, R. E. (1972). A general two-site solution for the chemical exchange produced
355 dependence of T2 upon the carr-Purcell pulse separation. *Journal of Magnetic Resonance (1969)*, 6(1), 89–

356 105. [https://doi.org/10.1016/0022-2364\(72\)90090-X](https://doi.org/10.1016/0022-2364(72)90090-X)

357 Chambers, J. M., Freeny, A., & Heiberger, R. M. (1992). Analysis of variance; designed experiments. In
358 *Statistical Models in S* (pp. 145–193). Wadsworth and Brooks/Cole Advanced Books and Software, Pacific
359 Grove, California.

360 Cleveland, W. S., Grosse, E., & Shyu, W. M. (1992). Local regression models. *Statistical Models in S*, 2, 309–
361 376. <https://doi.org/10.2307/1269676>

362 Conforti, P. A., Lupano, C. E., Malacalza, N. H., Arias, V., & Castells, C. B. (2006). Crystallization of honey at
363 -20°C. *International Journal of Food Properties*, 9(1), 99–107.
364 <https://doi.org/10.1080/10942910500473962>

365 Conover, W. J., & Iman, R. L. (1981). Rank transformations as a bridge between parametric and nonparametric
366 statistics. *American Statistician*, 35(3), 124–128. <https://doi.org/10.1080/00031305.1981.10479327>

367 Dettori, A., Tappi, S., Piana, L., Dalla Rosa, M., & Rocculi, P. (2018). Kinetic of induced honey crystallization
368 and related evolution of structural and physical properties. *LWT*, 95, 333–338.
369 <https://doi.org/10.1016/j.lwt.2018.04.092>

370 DIN-NORM-10758. (1997). Analysis of honey; determination of the content of saccharides fructose, glucose,
371 saccharose, turanose and maltose; HPLC method. Deutsches Institut für Normierung (1997--05) Berlin;
372 Germany.

373 Dobre, I., Georgescu, L. A., Alexe, P., Escuredo, O., & Seijo, M. C. (2012). Rheological behavior of different
374 honey types from Romania. *Food Research International*, 49(1), 126–132.
375 <https://doi.org/10.1016/j.foodres.2012.08.009>

376 Dunn, K. J. (2002). Enhanced transverse relaxation in porous media due to internal field gradients. *Journal of*
377 *Magnetic Resonance*, 156(2), 171–180. <https://doi.org/10.1006/jmre.2002.2541>

378 Dyce, E. J. (1935). 1,987,893. US patent.

379 Fabri, D., Williams, M. A. K., & Halstead, T. K. (2005). Water T2 relaxation in sugar solutions. *Carbohydrate*
380 *Research*, 340(5), 889–905. <https://doi.org/10.1016/j.carres.2005.01.034>

381 Gleiter, R. A., Horn, H., & Isengard, H. D. (2006). Influence of type and state of crystallisation on the water
382 activity of honey. *Food Chemistry*, 96(3), 441–445. <https://doi.org/10.1016/j.foodchem.2005.03.051>

383 Gonnet, M. (1994). La cristallisation dirigée des miels: actualization des méthodes de travail et avantages liés a

- 384 cette pratique technologique. *Abeilles & Fleurs*, 430, 12.
- 385 Hartel, R. W. (1993). Controlling Sugar Crystallization in Food Products. *Food Technology*, 47(11), 99–107.
386 <https://doi.org/10.1080/10408399109527541>
- 387 Hills, B. (1998). *Magnetic Resonance Imaging in Food Science*. (Wiley, Ed.). London: Wiley.
- 388 Hills, B. P., & Pardoe, K. (1995). Proton and deuterium NMR studies of the glass transition in a 10% water-
389 maltose solution. *Journal of Molecular Liquids*, 63(3), 229–237. [https://doi.org/10.1016/0167-](https://doi.org/10.1016/0167-7322(95)00796-D)
390 7322(95)00796-D
- 391 Hills, B. P., Wright, K. M., & Belton, P. S. (1989). Proton N.M.R. Studies of chemical and diffusive exchange in
392 carbohydrate systems. *Molecular Physics*, 67(6), 1309–1326. <https://doi.org/10.1080/00268978900101831>
- 393 Hubert, M., Rousseeuw, P. J., & Vanden Branden, K. (2005). ROBPCA: A new approach to robust principal
394 component analysis. *Technometrics*, 47(1), 64–79. <https://doi.org/Doi.10.1098/004017004000000563>
- 395 Iaccheri, E., Laghi, L., Cevoli, C., Berardinelli, A., Ragni, L., Romani, S., & Rocculi, P. (2015). Different
396 analytical approaches for the study of water features in green and roasted coffee beans. *Journal of Food*
397 *Engineering*, 146. <https://doi.org/10.1016/j.jfoodeng.2014.08.016>
- 398 Karasu, S., Toker, O. S., Yilmaz, M. T., Karaman, S., & Dertli, E. (2015). Thermal loop test to determine
399 structural changes and thermal stability of creamed honey: Rheological characterization. *Journal of Food*
400 *Engineering*, 150, 90–98. <https://doi.org/10.1016/j.jfoodeng.2014.10.004>
- 401 Laghi, L., Cremonini, M. A., Placucci, G., Sykora, S., Wright, K., & Hills, B. (2005). A proton NMR relaxation
402 study of hen egg quality. *Magnetic Resonance Imaging*, 23(3). <https://doi.org/10.1016/j.mri.2004.12.003>
- 403 Mauro, M. A., Dellarosa, N., Tylewicz, U., Tappi, S., Laghi, L., Rocculi, P., & Rosa, M. D. (2016). Calcium and
404 ascorbic acid affect cellular structure and water mobility in apple tissue during osmotic dehydration in
405 sucrose solutions. *Food Chemistry*, 195, 19–28. <https://doi.org/10.1016/j.foodchem.2015.04.096>
- 406 Meiboom, S., & Gill, D. (1958). Modified spin-echo method for measuring nuclear relaxation times. *Review of*
407 *Scientific Instruments*. <https://doi.org/10.1063/1.1716296>
- 408 Petracci, M., Laghi, L., Rimini, S., Rocculi, P., Capozzi, F., & Cavani, C. (2014). Chicken breast meat marinated
409 with increasing levels of sodium bicarbonate. *Journal of Poultry Science*, 51(2), 0130079.
410 <https://doi.org/10.2141/jpsa.0130079>
- 411 Petracci, M., Laghi, L., Rocculi, P., Rimini, S., Panarese, V., Cremonini, M. A., & Cavani, C. (2012). The use of

- 412 sodium bicarbonate for marination of broiler breast meat. *Poultry Science*, 91(2), 526–534.
 413 <https://doi.org/10.3382/ps.2011-01753>
- 414 R Development Core Team, R. (2011). *R: A Language and Environment for Statistical Computing*. R
 415 *Foundation for Statistical Computing* (Vol. 1). <https://doi.org/10.1007/978-3-540-74686-7>
- 416 Ribeiro, R. de O. R., Mársico, E. T., Carneiro, C. D. S., Monteiro, M. L. G., Júnior, C. C., & Jesus, E. F. O. De.
 417 (2014). Detection of honey adulteration of high fructose corn syrup by Low Field Nuclear Magnetic
 418 Resonance (LF 1H NMR). *Journal of Food Engineering*, 135, 39–43.
 419 <https://doi.org/10.1016/j.jfoodeng.2014.03.009>
- 420 Ribeiro, R. de O. R., Mársico, E. T., Carneiro, C. da S., Monteiro, M. L. G., Conte Júnior, C. A., Mano, S., & de
 421 Jesus, E. F. O. (2014). Classification of Brazilian honeys by physical and chemical analytical methods and
 422 low field nuclear magnetic resonance (LF 1H NMR). *LWT - Food Science and Technology*, 55(1), 90–95.
 423 <https://doi.org/10.1016/j.lwt.2013.08.004>
- 424 Serra-Bonvehí, J. (1974). La cristallisation du miel. Facteurs qui l’affecten. *Bullettin Technique Apicole*, 54(13),
 425 37–48.
- 426 Venir, E., Spaziani, M., & Maltini, E. (2010). Crystallization in “Tarassaco” Italian honey studied by DSC. *Food*
 427 *Chemistry*, 122(2), 410–415. <https://doi.org/10.1016/j.foodchem.2009.04.012>
- 428 Venturi, L., Rocculi, P., Cavani, C., Placucci, G., Dalla Rosa, M., & Cremonini, M. A. (2007). Water absorption
 429 of freeze-dried meat at different water activities: A multianalytical approach using sorption isotherm,
 430 differential scanning calorimetry, and nuclear magnetic resonance. *Journal of Agricultural and Food*
 431 *Chemistry*, 55(26), 10572–10578. <https://doi.org/10.1021/jf072874b>
- 432 Zamora, M. C., & Chirife, J. (2006). Determination of water activity change due to crystallization in honeys
 433 from Argentina. *Food Control*, 17(1), 59–64. <https://doi.org/10.1016/j.foodcont.2004.09.003>

436 **Figures Captions**

437 Figure 1: Relationship between enthalpy and storage time for static (continuous lines) and dynamic
438 (dashed lines) crystallization, for FC (points), MC (squares) and SC (triangles) samples.

439 Fig. 2. Relative concentration and T_2 of the two protons populations non-exchangeable and
440 exchangeable with water, as calculated from T_2 weighted curves obtained by TD-NMR on samples
441 stored statically (empty symbols) or dynamically (filled symbols) for fast (black circles), medium (dark
442 gray squares) and slow (light gray triangles) crystalizing samples. To ease visual inspection of the data,
443 trend dashed lines have been added for samples stored statically, while only samples at T_0 and T_f have
444 been represented for samples stored dynamically.

445 Figure 3: rPCA model calculated on the centered and scaled points of the T_2 weighted TD-NMR
446 signals. A) Scoreplot of samples stored statically (empty symbols) or dynamically (filled symbols) for
447 fast (black circles), medium (dark gray squares) and slow (light gray triangles) crystalizing samples. To
448 ease visual inspection of the data, for samples stored statically trend dashed lines have been added,
449 while for samples stored dynamically only data from T_0 and T_f have been represented. B) Example of
450 T_2 weighted TD-NMR signals, registered on FC samples at the beginning (black) and at the end (gray)
451 of the storage period. C) Correlation between the points of the signals and their importance over PC1

Declaration of interests

☒ The authors declare that they have no known competing financial interests or personal relationships that could have appeared to influence the work reported in this paper.

☐ The authors declare the following financial interests/personal relationships which may be considered as potential competing interests:

Table 1. Composition (g/100 g) of samples.

	Fructose	Glucose	Sucrose	Turanose	Maltose	Water	F/G
FCs	39.2	36.2	< 0.5	0.8	1.4	17.7	1.08
MCs	38.6	32.5	0.5	0.8	1.1	16.5	1.19
SCs	42.8	31.0	< 0.5	1.4	0.7	16.8	1.38
FCd	39.0	36.4	<0.5	0.9	1.2	16.0	1.07
MCd	39.7	32.9	<0.5	1.3	1.1	17.5	1.21
SCd	38.0	27.1	<0.5	1.1	0.6	17.3	1.4

Table 2. Main features of the crystallization kinetics observed through melting enthalpy.

	T ₀ static	T ₀ dynamic	Inflection point static		T _f static		T _f dynamic	
	Enthalpy *	Enthalpy	Enthalpy	Days	Enthalpy	Days	Enthalpy	Days
FC	4.32 ^a	3.72 ^{ab}	25.05 ^a	9	34.72 ^{ab}	50	38.01 ^a	10
MC	3.84 ^{ab}	5.09 ^a	16.31 ^{ab}	15	27.62 ^{bc}	90	31.39 ^b	16
SC	2.62 ^b	3.6 ^b	14.77 ^b	21	21.68 ^c	102	21.85 ^c	35

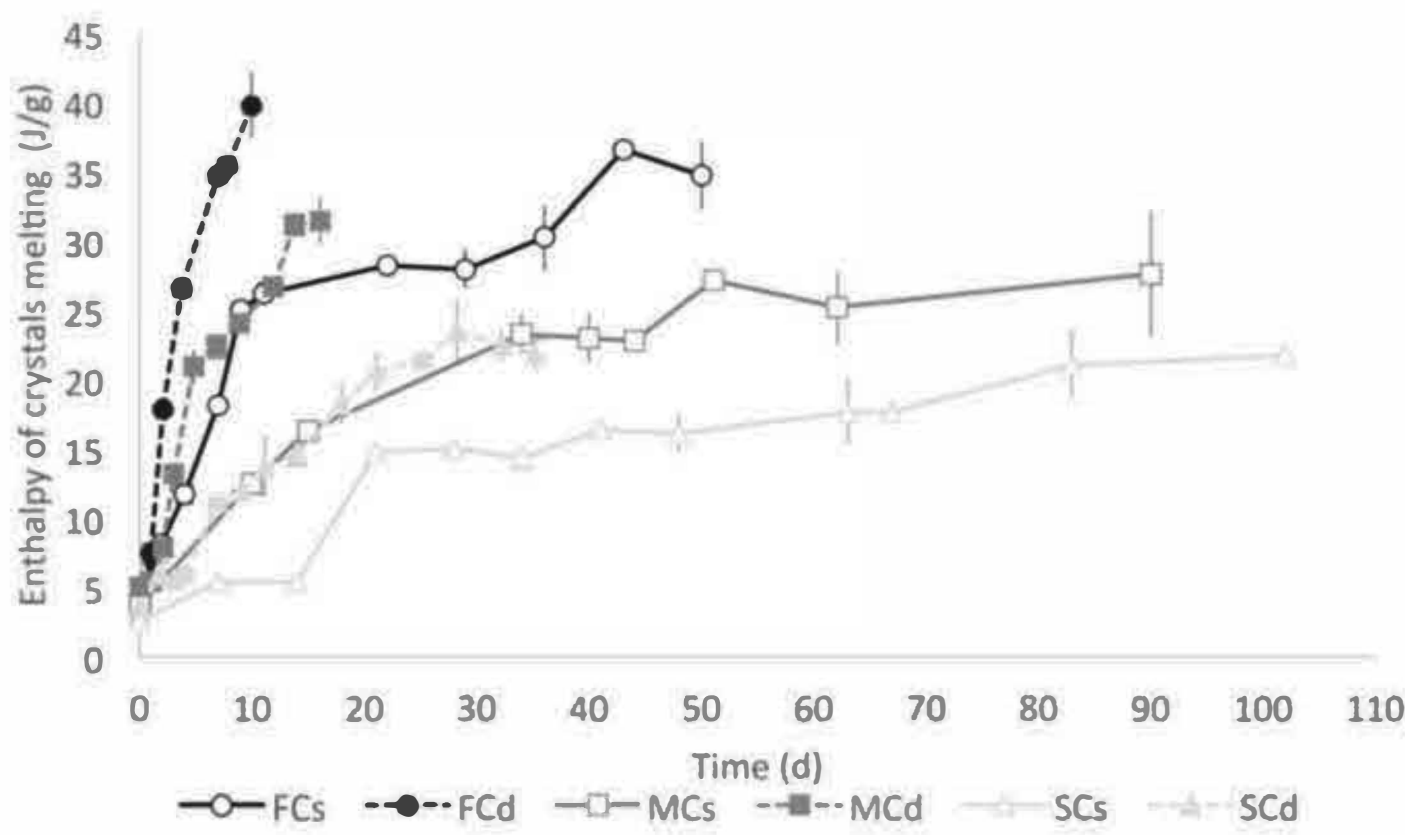
* Enthalpy is expressed in J/g. At each time-point, different letters indicate significant differences between samples. For readability, data dispersion is not indicated.

Table 3. For TD-NMR data, main features of the trends evidenced by the non-parametric fitting (dashed lines of figure 2).

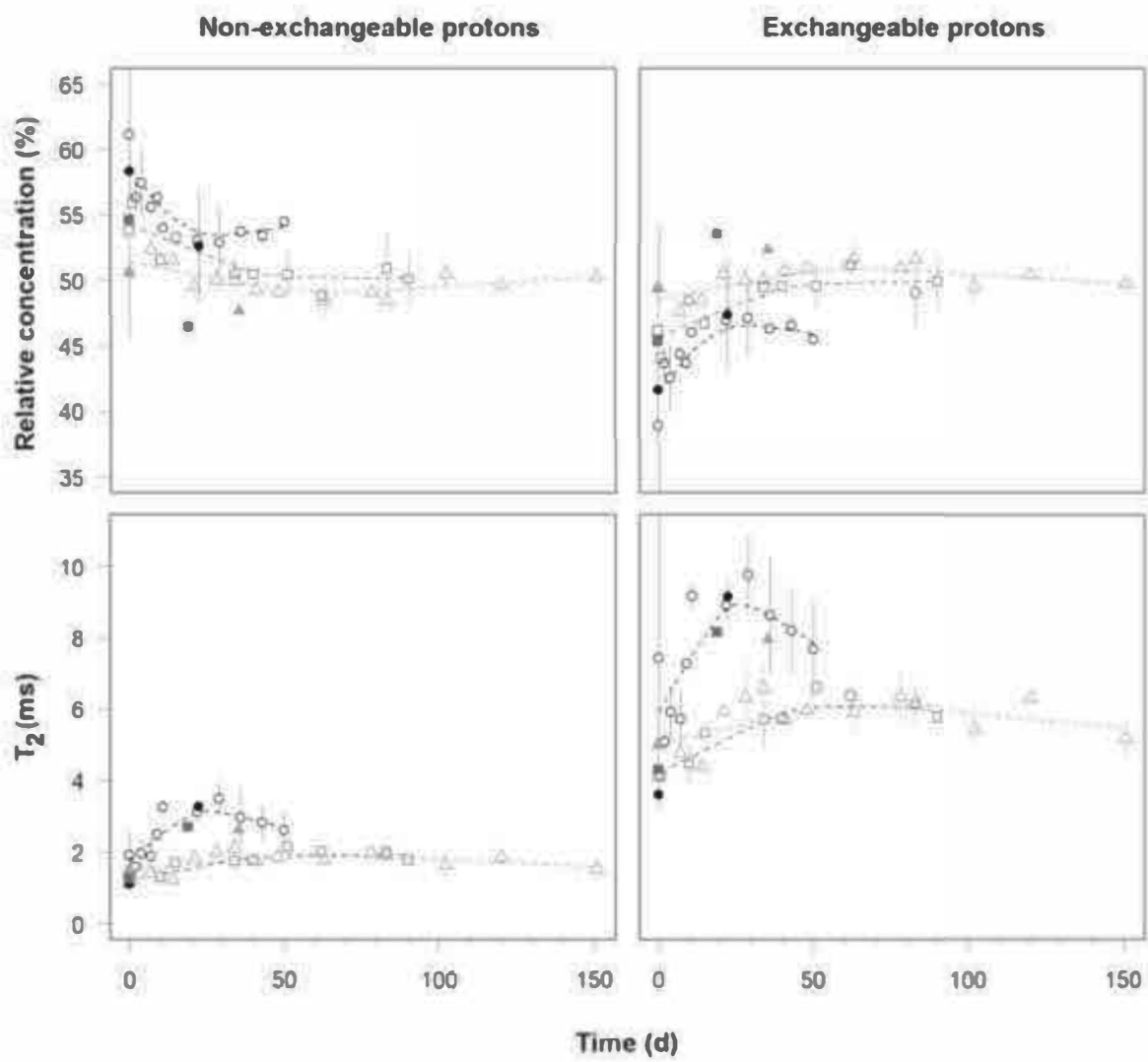
		T ₀ static		T ₀ dynamic		Inflection point static			T _f static		T _f dynamic	
		Int. %	T ₂ *	Int %	T ₂	Int. %	T ₂	Days	Int. %	T ₂	Int. %	T ₂
Non-exchangeable	FC	58.57 ^a	1.73 ^a	58.35 ^a	1.10 ^b	53.46 ^a	3.13 ^a	30	54.11 ^a	2.68 ^a	52.63 ^a	3.28 ^a
	MC	54.27 ^a	1.23 ^a	54.65 ^{ab}	1.26 ^b	50.15 ^b	1.93 ^b	50	50.15 ^b	1.93 ^a	46.47 ^b	2.70 ^b
	SC	51.47 ^b	1.48 ^a	50.63 ^b	1.50 ^a	49.12 ^b	1.87 ^b	66	50.28 ^b	1.59 ^a	47.68 ^{ab}	2.61 ^b
Exchangeable	FC	41.43 ^b	5.91 ^a	41.65 ^b	3.61 ^c	46.54 ^b	8.92 ^a	30	45.89 ^b	7.85 ^a	47.37 ^b	9.15 ^a
	MC	45.73 ^b	4.21 ^a	45.35 ^{ab}	4.31 ^b	49.85 ^b	6.10 ^b	50	49.85 ^a	6.09 ^a	53.53 ^a	8.15 ^b
	SC	48.53 ^a	4.96 ^a	49.37 ^a	5.01 ^a	50.88 ^a	6.04 ^b	66	49.72 ^a	5.48 ^a	52.32 ^{ab}	7.95 ^b

* T₂ values are expressed in ms. For readability, data dispersion is not indicated.

Figure(s)



Figure(s)



Figure(s)

